Communication

Bidirectional Electron Transfer in Photosystem I: Direct Evidence from High-Frequency Time-Resolved EPR Spectroscopy

Oleg G. Poluektov, Sergei V. Paschenko, Lisa M. Utschig, K. V. Lakshmi, and Marion C. Thurnauer

J. Am. Chem. Soc., **2005**, 127 (34), 11910-11911• DOI: 10.1021/ja053315t • Publication Date (Web): 04 August 2005

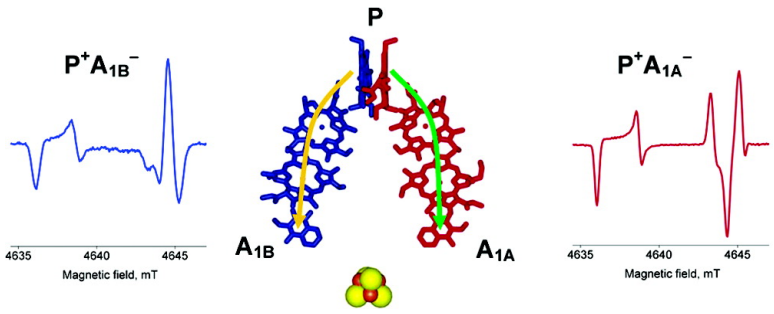

More About This Article

Additional resources and features associated with this article are available within the HTML version:

- Supporting Information
- Links to the 4 articles that cite this article, as of the time of this article download
- Access to high resolution figures
- Links to articles and content related to this article
- Copyright permission to reproduce figures and/or text from this article

View the Full Text HTML

J|A|C|S
COMMUNICATIONS

Published on Web 08/04/2005

Bidirectional Electron Transfer in Photosystem I: Direct Evidence from High-Frequency Time-Resolved EPR Spectroscopy

Oleg G. Poluektov,*,† Sergei V. Paschenko,† Lisa M. Utschig,† K. V. Lakshmi,‡ and Marion C. Thurnauer†

Chemistry Division, Argonne National Laboratory, 9700 South Cass Avenue, Argonne, Illinois 60439, and Department of Chemistry, CUNY Campus of Staten Island, 2800 Victory Boulevard, Staten Island, New York 10314

Received May 20, 2005; E-mail: oleg@anl.gov

The efficient charge separation that occurs within integral membrane reaction center (RC) proteins is the most important step of photosynthetic solar energy conversion. Although classified into two types, type I and type II, all RCs consist of a dimeric core, where each polypeptide binds a branch of cofactors (Figure 1). From the primary electron donor, P, which is a dimer of chlorophyll molecules, these two nearly symmetrical potential electron-acceptor chains (A and B branches) extend across the membrane. Anoxygenic photosynthesis of photosynthetic bacteria occurs in both types I and II RCs, whereas oxygenic photosynthesis of higher plants, cyanobacteria, and algae requires the symbiotic linking of types II and I RCs (photosystem II and photosystem I, respectively).[1]

Determining the functional roles for the pairs of cofactor branches is fundamental for understanding both the evolution of photosynthesis and the mechanisms of photosynthetic charge separation. In type II RCs, e.g., photosystem II (PSII), light-driven primary electron-transfer (ET) reactions take place exclusively through the A branch of redox-active components (unidirectional ET),[2] resulting in the charge-separated state, $P^+Q_A^-$, where Q_A^- is the reduced quinone cofactor in the A branch. Subsequently, ET proceeds from Q_A^- to the terminal electron acceptor, Q_B, the quinone cofactor in the B branch. Q_B is a mobile electron carrier. Following two proton-coupled electron-transfer events, Q_B is reduced to a hydroquinone and leaves the RC (Figure 1).

In photosystem I (PSI), photoexcitation of P initiates sequential ET through two spectroscopically identified electron acceptors, A_0, a chlorophyll molecule, and A_1, a phylloquinone. From A_1^- the electron is transferred to the [4Fe−4S] cluster F_X, and further to F_A and F_B, two iron−sulfur clusters held within an extrinsic protein subunit (Figure 1).[3] Thus, unlike that in type II RCs, ET in PSI does not terminate at two functionally distinct quinones, and the question of whether ET in PSI proceeds through both potential ET chains is currently under intense debate.

Experimental reports that address the directionality of ET are based on optical and time-resolved (TR) EPR studies of ET in wild-type PSI and site-directed mutants.[4−7] Two characteristic room-temperature ET rates from A_1^- to F_X, 5−10 ns and 150−200 ns, can be observed in these systems.[4] Without concomitant structural evidence, kinetic data is open to multiple interpretations. One interpretation of these observations favors unidirectional ET through the A branch and assumes that PSI has two conformational substates that exhibit different kinetics.[7] A second interpretation supports a bidirectional ET model in which the 5−10 ns kinetic component corresponds to ET through the B branch, while the 150−200 ns component is associated with ET through the A branch.[4−6]

Here we report the observation of two distinct transient spectra of $P^+A_1^-$ spin-correlated radical pairs (SCRPs) from the PSI RC protein of the cyanobacterium *Synechococcus lividus* using high-frequency (HF) TR-EPR methods. The application of advanced HF EPR techniques[8] having superior spectral resolution allows us to distinguish different geometries of the two SCRPs[9,10] and correlate their structures with kinetic data and the X-ray crystal structure of PSI.[3]

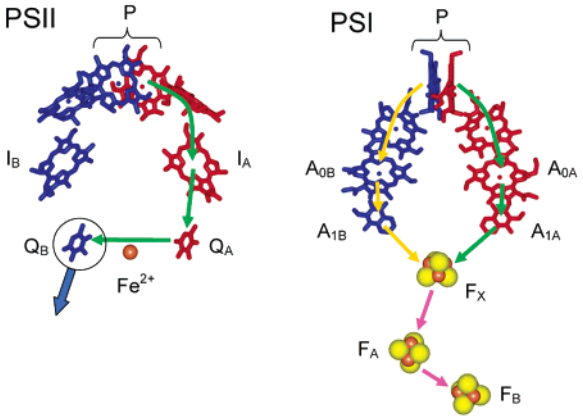

Figure 1. The potential ET cofactors in PSII (type II) and PSI (type I) photosynthetic reaction center proteins are arranged in two symmetric branches, A (red) and B (blue). In **PSII** photoinitiated ET is unidirectional through the A branch (green arrows). Whether photoinitiated electron transfer in **PSI** reaction centers occurs only along the A branch (green arrows) or along both the A and B branches (green and yellow arrows) is under debate.

To facilitate observation of the transient SCRP $P^+A_1^-$, we employed established methods for blocking ET by (photo)chemical reduction of the electron acceptors in PSI.[5,11] (See Supporting Information for the details of sample preparation and experimental conditions.) EPR signals of the stable radical species that result from these procedures will be discussed in a forthcoming publication. Here we concentrate only on transient SCRP states.

The light-induced HF TR-EPR signal observed from the dark-adapted PSI sample containing sodium ascorbate (Figure 2A) has a line shape which is similar to that of reported HF TR-EPR signals from the $P^+A_1^-$ SCRP in PSI.[9] The electron spin-polarization of this signal decays with a time constant of 60 μs (Figure 2C). This signal is due to ET through the A-branch where the ET beyond A_{1A} is blocked at 100 K, and thus, the reversibly formed $P^+A_{1A}^-$ SCRP is observed.[6,11]

The light-induced HF TR-EPR spectrum of PSI samples containing sodium hydrosulfite that were pre-illuminated at 205−245 K consists of EPR signals from several transient species (see Supporting Information). Fortunately, all of these EPR signals have different formation and decay kinetics, and this allows us to distinguish them and separate the contribution from the SCRP $P^+A_1^-$. The SCRP spectrum from the sample which was pre-illuminated for 1 h at 240 K, is presented in Figure 2B. Spin-polarization of this SCRP signal decays with a time constant of 6

† Argonne National Laboratory.
‡ CUNY Campus of Staten Island.

10.1021/ja053315t CCC: $30.25

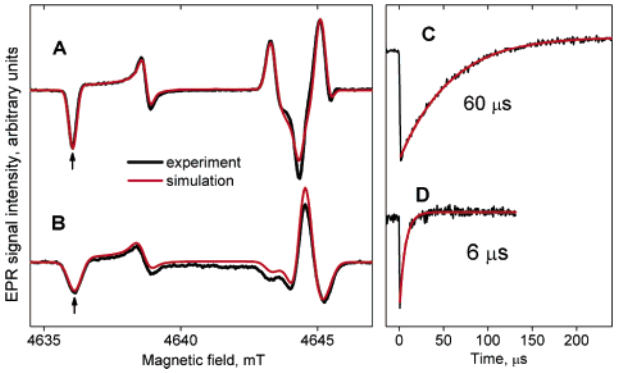

Figure 2. HF TR-EPR spectra of PSI complexes from perdeuterated cyanobacterium *S. lividus* at 100 K. (A, C) Sample with sodium ascorbate, dark-adapted; spectrum (A) corresponds to SCRP in the A branch, $P^+A_{1A}^-$. (B, D) Sample with sodium hydrosulfite, pre-illuminated at 240 K; spectrum (B) is assigned to $P^+A_{1B}^-$ in B branch. Decay kinetics (C) and (D) are recorded at quinones' g_X field positions, marked with arrows in (A) and (B), respectively. Difference in the line widths of the spectra in (A) and (B) is due to different detection bandwidths.

Table 1. Magnetic and Structural Parameters Used for the Simulations Shown in Figure 2

	magnetic interactions[a]		interspin vector direction in **g**-tensor axes of P^+		interspin vector direction in **g**-tensor axes of A_1^-	
	D, mT	J, μT	φ[c]	θ[c]	φ[c]	θ[c]
$P^+A_{1A}^-$	−0.17[b]	2	118°	39°	0°	79°
$P^+A_{1B}^-$	−0.17[b]	2	128°	90°	1°	88°

	g-tensor principal values,[d] $(g_i - 2) \times 10^4$; where $i = X, Y, Z$		
	g_X	g_Y	g_Z
P^+	32.2	27.7	24.6
A_{1A}^-	63.6[e]	52.0	23.1
A_{1B}^-	62.9[e]	52.0	23.1

[a] D - dipolar, J - exchange interaction. [b] References 6,13. [c] φ - azimuthal, θ - tangential angle. [d] Absolute values are calibrated so that g_Z of P^+ is equal to that in ref 12. [e] Ref 14.

μs (Figure 2D). For shorter pre-illumination times, the SCRP spectrum is a mixture of those presented in Figure 2, A and B, and exhibits biexponential decay times of 60 and 6 μs.

The different line shapes of the SCRP spectra shown in Figure 2, A and B, indicate a difference in the geometry of these two radical pairs. We suggest that the transient spectrum in Figure 2B can be assigned to a SCRP in the B branch, $P^+A_{1B}^-$. Addition of sodium hydosulfite and pre-illumination leads to reduction of F_X, F_A and F_B and thus blocks ET beyond A_{1B}.[5,6] The absence of the 60-μs component after long pre-illumination times (Figure 2D) could then be explained by complete reduction of A_{1A}, either singly or doubly, so that the ET to A_{1A} is completely blocked. In accord with the model presented by Heathcote and Evans,[5,6] $P^+A_{1B}^-$ does not contribute to the spectrum from the sodium ascorbate-containing sample (Figure 2A) because in this case, F_X is not reduced, and electron transfer along the B chain proceeds beyond A_{1B} to generate $P^+F_X^-$, $P^+F_A^-$, and $P^+F_B^-$ states.

Supporting evidence for the direct observation of the two SCRPs $P^+A_{1A}^-$ and $P^+A_{1B}^-$ from the A and B branches, respectively, is provided by the fact that the spectra for both SCRPs can be simulated *simultaneously* (Figure 2, A and B) using the same magnetic but different geometric parameters (Table 1 and Supporting Information), where the latter are taken from the X-ray crystal structure.[3] The difference in line shapes between the two SCRP spectra assigned to $P^+A_{1A}^-$ and $P^+A_{1B}^-$, particularly at the high-field portions, can be understood within the model developed for SCRP EPR spectra in the limit of weak dipolar interactions.[10] In PSI, the orientations of the quinones are highly symmetric relative to the quinone-primary donor interconnection vectors.[3] This symmetry determines the similar line shapes of the low-field parts, where the main contribution is from the quinone member of the SCRP. The distinctions between the high-field region of the spectra, where the main contribution is from P^+, indicates that the directions of the $P^+ - A_{1A}^-$ and $P^+ - A_{1B}^-$ interspin vectors, as expected,[7e,9] are not symmetric relative to the **g**-tensor principal axes of P^+.

In summary, we report the direct observation of two SCRPs in PSI arising from both the A and B branches of ET cofactors. The geometry of the SCRPs, derived from the simulation of the HF TR-EPR spectra, is in excellent agreement with the X-ray crystal structure of PSI. The concomitant structural and kinetic information obtained with HF EPR provide unambiguous evidence of ET only along the B branch in PSI at low temperature and under strongly reducing conditions. These findings, together with previously reported data on the PSI mutants and wild-type proteins,[4−6] are consistent with bidirectional ET in PSI.

Acknowledgment. This work was supported by the U.S. Department of Energy, Office of Basic Energy Sciences, Division of Chemical Sciences, Geosciences, and Biosciences, under Contract W-31-109-Eng-38.

Supporting Information Available: Sample preparation procedures, experimental details and high-frequency TR EPR spectra. This material is available free of charge via the Internet at http://pubs.acs.org.

References

(1) Barber, J.; Archer, M. D. *J. Photochem. Photobiol., A* **2001**, *142*, 97−106.
(2) Heller, B. A.; Holten, D.; Kirmaier, C. *Science* **1995**, *269*, 940−945.
(3) Jordan, P.; Fromme, P.; Witt, H. T.; Klukas, O.; Saenger, W.; Krauss, N. *Nature* **2001**, *411*, 909−917.
(4) (a) Joliot, P.; Joliot, A. *Biochemistry* **1999**, *38*, 11130−11136. (b) Guergova-Kuras, M.; Boudreaux, B.; Joliot, A.; Joliot, P.; Redding, K. *Proc. Natl. Acad. Sci. U.S.A.* **2001**, *98*, 4437−4442.
(5) Muhiuddin, I. P.; Heathcote, P.; Carter, S.; Purton, S.; Rigby, S. E. J.; Evans, M. C. W. *FEBS Lett.* **2001**, *503*, 56−60.
(6) Santabarbara, S.; Kuprov, I.; Fairclough, W. V.; Purton, S.; Hore, P. J.; Heathcote, P.; Evans, M. C. W. *Biochemistry* **2005**, *44*, 2119−2128.
(7) (a) Xu, W. et al. *J. Biol. Chem.* **2003**, *278*, 27876−27887. (b) Cohen, R. O.; Shen, G. Z.; Golbeck, J. H.; Xu, W.; Chitnis, P. R.; Valieva, A. I.; van der Est, A.; Pushkar, Y.; Stehlik, D. *Biochemistry* **2004**, *43*, 4741−4754. (c) Dashdorj, N.; Xu, W.; Cohen, R. O.; Golbeck, J. H.; Savikhin, S. *Biophys. J.* **2005**, *88*, 1238−1249. (d) Shen, G. Z. et al. *J. Biol. Chem.* **2002**, *277*, 20355−20366. (e) Wyndhamn, I.; van der Est, A.; Stehlik, D.; Cohen, R.; Golbeck J. In *Photosynthesis: Fundamental Aspects to Global Perspectives*; van der Est, A., Bruce, D., Eds.; Alliance Communications Group: Lawrence, KS, 2005; pp 88−90.
(8) *Very High Frequency (VHF) ESR/EPR*; Grinberg, O., Berliner, L. J., Eds.; Biological Magnetic Resonance, Vol. 22; Kluwer Academic/Plenum Publishers: New York, 2004.
(9) (a) van der Est, A.; Prisner, T.; Bittl, R.; Fromme, P.; Lubitz, W.; Mobius, K.; Stehlik, D. *J. Phys. Chem. B* **1997**, *101*, 1437−1443. (b) Zech, S. G.; Hofbauer, W.; Kamlowski, A.; Fromme, P.; Stehlik, D.; Lubitz, W.; Bittl, R. *J. Phys. Chem. B* **2000**, *104*, 9728−9739. (c) Link, G.; Berthold, T.; Bechtold, M.; Weidner, J.-U.; Ohmes, E.; Tang, J.; Poluektov, O.; Utschig, L.; Schlesselman, S. L.; Thurnauer, M. C.; Kothe, G. *J. Am. Chem. Soc.* **2001**, *123*, 4211−4222.
(10) (a) Kandrashkin, Y.; van der Est, A. *Spectrochim. Acta A* **2001**, *57*, 1697−1709. (b) Dubinski, A. A.; Perekhodtsev, G. D.; Poluektov, O. G.; Rajh, T.; Thurnauer, M. C. *J. Phys. Chem. B* **2002**, *106*, 938−944.
(11) Schlodder, E.; Falkenberg, K.; Gergeleit, M.; Brettel, K. *Biochemistry* **1998**, *37*, 9466−9476.
(12) Poluektov, O. G.; Utschig, L. M.; Schlesselman, S. L.; Lakshmi, K. V.; Brudvig, G. W.; Kothe, G.; Thurnauer, M. C. *J. Phys. Chem. B* **2002**, *106*, 8911−8916.
(13) (a) Bittl, R.; Zech, S. G. *J. Phys. Chem. B* **1997**, *101*, 1429−1436. (b) Dzuba, S. A.; Hara, H.; Kawamori, A.; Iwaki, M.; Itoh, S.; Tsvetkov, Y. D. *Chem. Phys. Lett.* **1997**, *264*, 238−244.
(14) The observed shift of the g_X component of A_1^- is similar to the shift in purple photosynthetic bacterial RCs for Q_B^- in comparison with Q_A^-, and reflects a similar trend in asymmetric H-bonding in PSI: only one carbonyl oxygen in A_{1A}^- has a strong H-bond, while in A_{1B}^- both carbonyl oxygens have strong H-bonds. (a) Lubitz, W.; Feher, G. *Appl. Magn. Reson.* **1999**, *17*, 1−48. (b) Sinnecker, S.; Reijerse, E.; Neese, F.; Lubitz, W. *J. Am. Chem. Soc.* **2004**, *126*, 3280−3290.

JA053315T